2011 IEEE International Conference on Rehabilitation Robotics
Rehab Week Zurich, ETH Zurich Science City, Switzerland, June 29 - July 1, 2011

Effects of Ankle Stiffness on Gait Selection of Dynamic Bipedal Walking with Flat Feet

Yan Huang, Qining Wang, Baojun Chen and Long Wang

***Abstract*— This paper investigates the effects of ankle joint stiffness on gait selection of dynamic bipedal walking with flat feet. We present a dynamic bipedal walking model with upper body, flat feet and compliant joints. The model can generate the three common gaits of dynamic bipedal walking. Simulation experiments are carried out to verify the analytical results and provide further results on gait comparison and selection.**

I. INTRODUCTION

Bipedal walking can be done in two biomechanical ways: dynamic gait where the center of gravity moves up and down as an inverted pendulum or static gait where the body's center of mass maintains in a constant position [1], [2]. Different from static walking, dynamic bipedal walkers which show a remarkable resemblance to the human gait may not reach equilibrium at every moment during motion, but can realize stable cyclic walking. As an example, passive dynamic walking [3] has been presented as a possible explanation for the efficiency of the human gait, which showed that a mechanism with two legs can be constructed so as to descend a gentle slope with no actuation and no active control.

Most studies of passive dynamic walking are based on the Simplest Walking Model proposed by [4] and extended work by [5], which consists of two rigid massless legs connected by a frictionless hinge at the hip, with a large point mass at the hip and a small mass at each foot (placed at the ankle). Recently, several flat-foot dynamic walking models are established to further study the bipedal locomotion [6], [7], [9], [10], [11]. Different from point-foot and round-foot walkers, dynamic bipedal walking with flat feet has multiple contact cases for each leg (heel contact, toe contact, full foot contact). Thus the walking sequence is not predetermined. Walking sequence of flat-feet walkers has several substreams, which result in various walking gaits. Comparison of motion performance of different walking gaits may explain why human normal walking is the optimal gait, and also provide evidences of the effect of body properties on gait selection, which help us better understand human walking. In addition to energetic efficiency, ankle stiffness may affect the gait selection of dynamic bipedal walking. However, no further study has been done.

To investigate the effects of ankle stiffness on gait selection, in this study, we establish a seven-link dynamic walking model that is more close to human beings. We add hip actuation, upper body, flat feet and torsional springs on ankle joints to the model. The cyclic walking is described as several phases, distinguished by the contact condition. Switching of walking phases is determined by the directions of ground reaction forces. Three typical walking gaits are realized by the proposed model. We evaluate the walking characteristics for each gait and investigate the effects of actuation mode and ankle stiffness on gait selection. Simulation experiments are carried out to verify the analytical results and provide further results on gait selection.

The rest of this paper is organized as follows. Section II presents the dynamic walking model with flat feet and joint compliance, and describes the walking phases and possible gaits of the proposed model. Section III shows the intrinsic reason which results in the difference of performance of the walking gaits. Section IV gives the simulation results. We conclude in Section V.

II. MODEL

A. Bipedal Model

To obtain further understanding of real human walking, we propose a passivity-based bipedal walking model that is more close to human beings. We add flat feet and compliant ankle joints to the model. As shown in Fig. 1, the two-dimensional

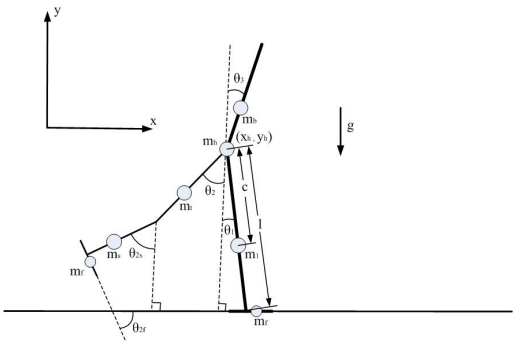

Fig. 1. Dynamic bipedal walking model with flat feet and compliant ankles.

model consists of two rigid legs interconnected individually through a hinge with a rigid upper body (mass added stick) connected at the hip. Each leg includes thigh, shank and foot. The thigh and the shank are connected at the knee joint, while the foot is mounted on the ankle with a torsional spring. A point mass at hip represents the pelvis. The mass of each leg and foot is simplified as point mass added on the Center of Mass (CoM) of the shank, the thigh, and the foot,

This work was supported by the National Natural Science Foundation of China (No. 61005082, 61020106005), Doctoral Fund of Ministry of Education of China (No. 20100001120005) and the 985 Project of Peking University (No. 3J0865600).

The authors are with the Intelligent Control Laboratory, College of Engineering, Peking University, Beijing 100871, China.
Email: Q. Wang (qiningwang@pku.edu.cn)

respectively. Similar to [12], a kinematic coupling has been used in the model to keep the body midway between the two legs. In addition, our model adds compliance to the knee joints and ankle joints. Specifically, knee joints and ankle joints are modeled as passive joints that are constrained by torsional springs. To simplify the motion, we have several assumptions, including 1) shanks and thighs suffering no flexible deformation; 2) hip joint and knee joints with no damping or friction; 3) the friction between the walker and the ground is enough. Thus the flat feet do not deform or slip; 4) strike is modeled as an instantaneous, fully inelastic impact where no slip and no bounce occurs. The bipedal walker travels forward on level ground with hip actuation.

The stance leg keeps contact with ground while the swing leg pivots about the constraint hip. When the flat foot strikes the ground, there are two impulses, "heel-strike" and " foot-strike", representative of the initial impact of the heel and the following impact as the whole foot contacts the ground [10]. The shank of the stance foot is always locked and the whole leg can be modeled as one rigid stick, while the knee joint of the swing leg will release the shank immediately after foot-strike. The shank will be locked when it swings forward to a relatively small angle to the thigh.

We suppose that the x-axis is along the ground while the y-axis is vertical to the ground upwards. The configuration of the walker is defined by the coordinates of the point mass on hip joint and several angles which include the swing angles between vertical coordinates and each thigh and shank, the angle between vertical coordinates and the upper body and the foot angles between horizontal coordinates and each foot (see Fig. 1 for details), which can be arranged in a generalized vector $q = (x_h, y_h, \theta_1, \theta_2, \theta_3, \theta_{2s}, \theta_{1f}, \theta_{2f})^T$. The positive directions of all the angles are counter-clockwise. Note that the dimension of the generalized vector in different phases may be different. When the knee joint of the swing leg is locked, the freedom of the shank is reduced and the angle θ_{2s} is not included in the generalized coordinates. Consequently, the dimensions of mass matrix and generalized active force are also reduced in some phases.

B. Walking Dynamics

In the following paragraphs, we will focus on the Equation of Motion (EoM) of the bipedal walking dynamics of the proposed model. The model can be defined by the rectangular coordinates x, which can be described by the x-coordinate and y-coordinate of the mass points (suppose leg 1 is the stance leg):

$$x = [x_h, y_h, x_{c1}, y_{c1}, x_{c2t}, y_{c2t}, x_{c3}, y_{c3}, x_{c2s}, y_{c2s}, x_{c1f}, y_{c1f}, x_{c2f}, y_{c2f}]^T \quad (1)$$

The walker can also be described by the generalized coordinates q as mentioned before:

$$q = (x_h, y_h, \theta_1, \theta_2, \theta_3, \theta_{2s}, \theta_{1f}, \theta_{2f})^T \quad (2)$$

We defined matrix T as follows:

$$T = dq/dx \quad (3)$$

Thus T transfers the independent generalized coordinates $\dot{q}$ into the velocities of the rectangular coordinates $\dot{x}$. The mass matrix in rectangular coordinate x is defined as:

$$M = diag(m_h, m_h, m_l, m_l, m_t, m_t, m_b, m_b, m_s, m_s, m_f, m_f, m_f, m_f) \quad (4)$$

Denote F as the active external force vector in rectangular coordinates. The constraint function is marked as $\xi(q)$, which is used to maintain foot contact with ground and detect impacts. Note that $\xi(q)$ in different walking phases may be different since the contact conditions change. The contact of stance foot is modeled by one ground reaction force (GRF) along the floor and two GRFs perpendicular to the ground act on the two endpoints of the foot, respectively. If one of the forces perpendicular to the ground decreases below zero, the corresponding endpoint of the stance foot will lose contact with ground and the stance foot will rotate around the other endpoint.

We can obtain the EoM by Lagrange's equations:

$$M_q \ddot{q} = F_q + \Phi^T F_f \quad (5)$$

$$\xi(q) = 0 \quad (6)$$

where $\Phi = \frac{\partial \xi}{\partial q}$. F_f is the constraint generalized force vector corresponding to the constraint function $\xi(q)$. M_q is the mass matrix in the generalized coordinates:

$$M_q = T^T M T \quad (7)$$

F_q is the active external force in the generalized coordinates:

$$F_q = T^T F - T^T M \frac{\partial T}{\partial q} \dot{q}\dot{q} \quad (8)$$

Equation (6) can be transformed to the followed equation:

$$\Phi \ddot{q} = -\frac{\partial(\Phi \dot{q})}{\partial q} \dot{q} \quad (9)$$

Then the EoM in matrix format can be obtained from Equation (5) and Equation (9):

$$\begin{bmatrix} M_q & -\Phi^T \\ \Phi & 0 \end{bmatrix} \begin{bmatrix} \ddot{q} \\ F_f \end{bmatrix} = \begin{bmatrix} F_q \\ -\frac{\partial(\Phi \dot{q})}{\partial q} \dot{q} \end{bmatrix} \quad (10)$$

The equation of strike moment can be obtained by integration of Equation (5):

$$M_q \dot{q}^+ = M_q \dot{q}^- + \Phi^T I_f \quad (11)$$

where $\dot{q}^+$ and $\dot{q}^-$ are the velocities of generalized coordinates just after and just before the strike, respectively. Here, I_f is the impulsive force acted on the walker which is defined as follows:

$$I_f = \lim_{t^- \to t^+} \int_{t^-}^{t^+} F_f dt \quad (12)$$

Since the strike is modeled as a fully inelastic impact, the walker satisfies the constraint function $\xi(q)$. Thus the motion is constrained by the followed equation after the strike:

$$\frac{\partial \xi}{\partial q} \dot{q}^+ = 0 \quad (13)$$

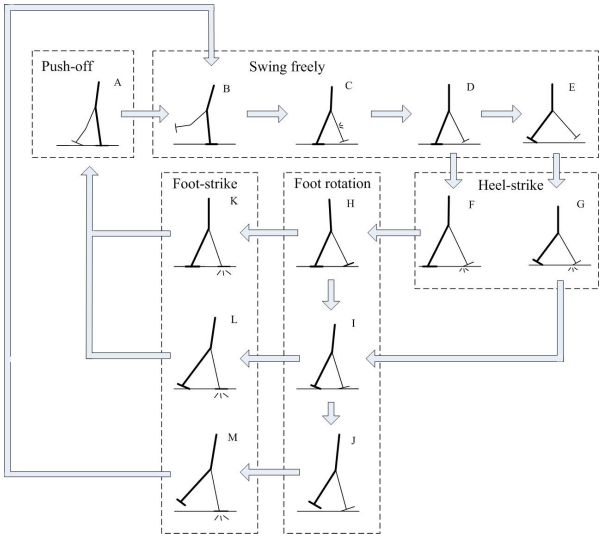

Fig. 2. Walking sequence of the passivity-based biped with flat feet and ankle compliance. The walking sequence has several sub-streams which indicate different gaits with corresponding walking phases.

Then the equation of strike in matrix format can be derived from Equation (11) and Equation (13):

$$\begin{bmatrix} M_q & -\Phi^T \\ \Phi & 0 \end{bmatrix} \begin{bmatrix} \dot{q}^+ \\ I_f \end{bmatrix} = \begin{bmatrix} M_q \dot{q}^- \\ 0 \end{bmatrix} \tag{14}$$

C. Walking Phases

The walking sequence of the flat-foot walker is more complicated than that of the round-foot walker [7], [10]. When the flat foot strikes the ground, there are two impulses, "heel-strike" and "foot-strike", representing the initial impact of the heel and the following impact as the whole foot contacts the ground. Each foot has three contact cases: foot contact, heel contact and toe contact. Thus there appears several sub-streams in the walking sequence (see Fig. 2). Note that one walking step may not include all the phases in Fig. 2. Moving to which phase at the bifurcation point is based on the contact force. The direction of the GRF perpendicular to the ground acted on the endpoint of the foot is checked at every simulation step during the motion. The corresponding contact condition is released if the force becomes downward. An impact happens when a new contact is detected. The directions of all the impulsive forces are checked. If an impulsive force is downward, the corresponding constraint is released and the impact is recalculated with the new constraint function.

D. Bipedal Walking Gaits

According to the walking sequence discussed above, the proposed bipedal model with flat feet and compliant joints has several possible cyclic walking gaits. Not that the walking sequence shown in Fig. 2 is an ideal case according to the multi-rigid body mechanics. Some of the walking gaits (for example, the gaits without the push-off phase) included in the sequence are rarely found in real human walking. Thus we ignore these gaits in this paper for their atypical performance. The three most commonly human walking gaits can be generated by the proposed bipedal model:

- Gait 1: "$A \rightarrow B \rightarrow C \rightarrow D \rightarrow F \rightarrow H \rightarrow K \rightarrow A$". The whole foot of the stance leg keeps contact with ground till the foot-strike of the swing leg occurs. This gait often has a very short step length.
- Gait 2: "$A \rightarrow B \rightarrow C \rightarrow D \rightarrow F \rightarrow H \rightarrow I \rightarrow L \rightarrow A$". The heel of the stance leg loses contact with ground before the foot-strike of the swing leg occurs. The step length of this gait is relatively small.
- Gait 3: "$A \rightarrow B \rightarrow C \rightarrow D \rightarrow E \rightarrow G \rightarrow I \rightarrow L \rightarrow A$". The heel of stance leg loses contact with ground before heel-strike of swing leg, which is called premature heel rise in [9]. This gait often has a relatively large step length.

Gait 1 with a short step length can be found in walking in a crowded queue. The step length is confined in a small range. Gait 2 and Gait 3 with moderate step lengths perform a great resemblance to human normal walking.

E. Actuation Mode

We add a piecewise constant hip torque to actuate the walker to travel forward on level ground. The hip torque may be different in different phases. The torque is relatively large in push-off phase and double-support phase to actuate the swing foot to leave ground and compensate the energy loss at heel-strike, and is near zero in the freely swing phase based on the fact that the muscles of the swing leg are generally silent [7], [8].

Torsional springs are added at ankle joints to represent ankle stiffness. Several studies indicate that ankle behavior in human walking is quite similar to that of a torsional spring [13], [14]. The ankle stiffness in human walking varies in one step [15]. To improve the performance of walking and achieve various walking gaits, we set different values of ankle stiffness during the stance phase, which shows a great resemblance with human normal walking [15] (see Fig. 3). Similar approaches have been used in recent studies [9].

In our biped walking model, the ankle stiffness has a larger value when the leg has passed the ground normal during the foot-flat phase. During the rest of the stance, the ankle stiffness is lower. In toe-down, foot-flat and swing phases ($O \rightarrow A$, $A \rightarrow O$ and $B \rightarrow C$ in Fig. 3(b)) the ankle joint reaches equilibrium position when the leg is vertical to foot. The equilibrium position has a deviation in push-off phase ($O \rightarrow B$ in Fig. 3(b)). The detailed expression is:

$$\begin{aligned} Tor &= K_a \cdot \phi, \text{ toe-down phase and foot-flat phase with the leg before mid-stance} \\ Tor &= K_b \cdot \phi, \text{ foot-flat phase with the leg passing mid-stance} \\ Tor &= K_a \cdot (\phi - \phi_0), \text{ push-off phase} \end{aligned} \tag{15}$$

where ϕ is the ankle angle, which is equal to $\theta_{2f} - \theta_{2s}$ for leg 2 in Fig. 1, and Tor is the torque generated by the ankle spring, which is positive when pulling up the heel. ϕ_0 is the equilibrium ankle angle in push-off phase. K_a, K_b and ϕ_0 may be different for different walking solutions.

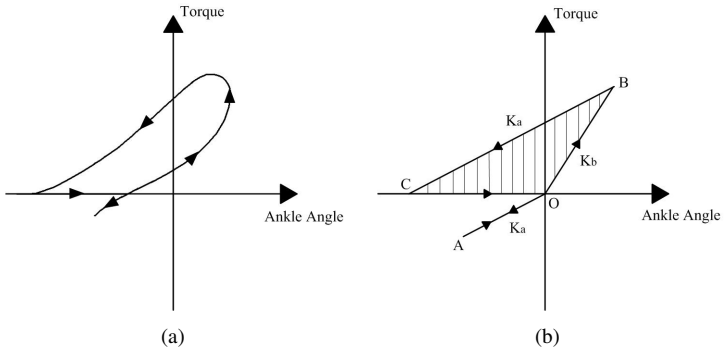

Fig. 3. Comparison of ankle behavior of human normal walking and the proposed model. (a) shows the torque-angle relationship in ankle joint of human normal walking, adapted from Frigo et al[13]. Ankle angle is the deviation of the foot angle from the direction orthogonal to the shank. y-axis is the ankle joint torque. (b) shows the torque-angle relationship in ankle joint of the proposed model. O (the origin point): Heel-strike; $O \rightarrow A$: Toe-down phase; $A \rightarrow O$: Foot-flat phase (the leg is before mid-stance. The ankle stiffness is K_a); $O \rightarrow B$: Foot-flat phase (the leg has passed mid-stance and the ankle stiffness has a larger value K_b.); $B \rightarrow C$: Push-off phase. The ankle stiffness return to K_a. The line BC is parallel to the line AO. ; $C \rightarrow O$: Swing phase, the foot is reset to the equilibrium position.

The ankle torque changes continuously at the switching of ankle stiffness, which means that the switching does not bring additional energy. The foot is supposed to be constrained vertically to the shank to avoid oscillation during swing phase. The ankle does a amount of net work as shown by the hatched area in Fig. 3(b), which is taken consider into the calculation of energetic efficiency.

In the following simulation, stable cyclic walking is searched for various combination of actuation pattern and ankle stiffness. The hip torques of the representatives of the three gaits are shown in Fig. 4. The two ankle stiffness values

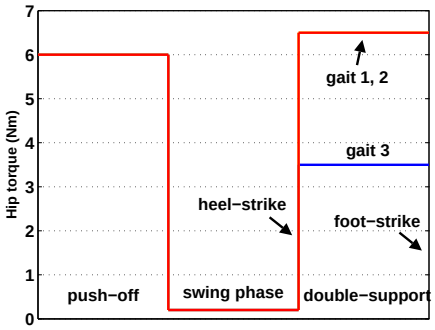

Fig. 4. Schematic diagram of the actuation patterns for the three gaits. Gait 1 and Gait 2 have the same pattern, described by the red lines, as the two gaits have a lot of similar characteristics. The hip torque of Gait 3 is different only for the double-support phase in this figure, illustrated by the blue lines.

of each gait are: Gait 1, $30Nm/rad$, $54Nm/rad$; Gait 2, $50Nm/rad$, $90Nm/rad$; Gait 3, $35Nm/rad$, $95Nm/rad$.

III. Experimental Results

In this section, we show the simulation experiments to investigate the effects of ankle stiffness on gait selection of dynamic bipedal walking. Based on the EoMs mentioned in Section II, we analyzed the walking motion of the biped. The numerical integration of the second order differential EoMs used the Runge-Kutta method. Parameters values used in the analysis are specified in Table I. All masses and lengths are normalized by total mass and leg length respectively.

TABLE I

Parameter values in simulations.

Parameter	Value
leg mass m_l	0.1538
thigh mass m_t	0.1077
shank mass m_s	0.0461
foot mass m_f	0.0355
upper body mass m_b	0.355
hip mass m_h	0.2663
leg length l	1
thigh length l_t	0.55
shank length l_s	0.45
foot length l_f	0.25
upper body length l_b	0.75
distance from ankle joint to heel l_{ah}	0.1
distance from hip joint to CoM of thigh c_t	0.2750
distance from knee joint to CoM of shank c_s	0.2250
distance from ankle joint to CoM of foot c_f	0.0250
distance from hip joint to CoM of upper body c_b	0.3750

A. Effects of Hip Torque

As the walker travels on the level ground, we add a hip torque to the biped model as the actuation. According to our experiments, stable cyclic walking is found when the torque has a larger value in push-off phases and double-support phases while a smaller value in freely swing phases, as mentioned above. To study the energy loss at heel-strike for different gaits, which relates to the actuation required in double-support phase, the motion characteristics of the three walking gaits are compared for different hip torques in double-support phases.

Fig. 5 shows the efficiency of the three gaits for different torques in double-support phases. The torque in push-off phase is fixed at $6.0Nm$ for all gaits. In this paper, the efficiency of the dynamic walking is measured by the nondimensional form of 'specific resistance' [12], which is the

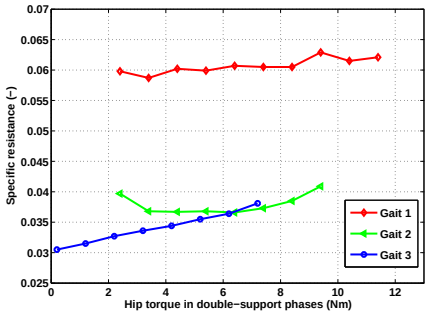

(a)

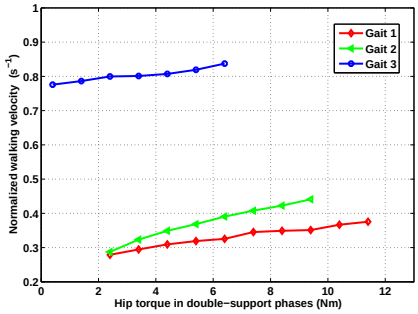

(b)

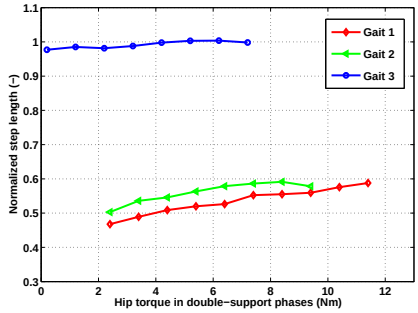

(c)

Fig. 5. (a)Efficiency, (b)walking velocity and (c)step length of the three gaits for different hip torques in double-support phases. The ankle stiffnesses are chosen as the typical values of each gait: Gait 1, $K_a = 35N/m$, $K_b = 70N/m$; Gait 2, $K_a = 80N/m$, $K_b = 110N/m$; Gait 3, $K_a = 45N/m$, $K_b = 95N/m$. The walking velocity and step length are normalized by the leg length.

energy consumption per kilogram mass per distance traveled per gravity. The results indicate that Gait 3 is the most efficient gait, while the energy consumption of Gait 1 is the largest. In addition, Gait 3 has both the largest velocity and the largest step length, and Gait 1 is the smallest one in these two aspects. One can also find that stable cyclic walking of Gait 1 and Gait 2 are distributed mainly over high range of hip torque, in contrast, Gait 3 is mainly found when the hip torque is relatively small. The results suggest that energy loss at heel-strike of Gait 3 is less than those of Gait 2 and Gait 1, and Gait 3 needs the least hip torque in double-support phase to compensate the energy loss. These experimental results are consistence with the analysis in Section II. Fig. 5 also reveals the effects of hip torque on the locomotion. Walking

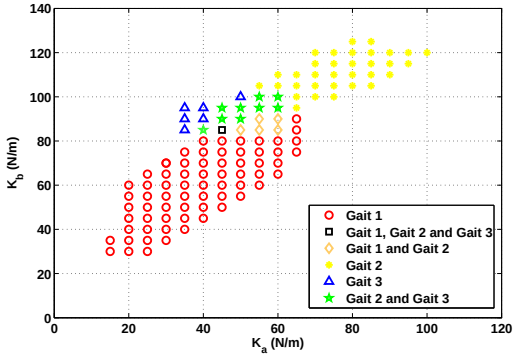

Fig. 6. Distribution of different walking gaits in the K_a-K_b plane. The hip torque in push-off phase for all the three gaits is $6.0Nm$. In the double-support phase, the hip torque of Gait 1 and Gait 2 is $6.5Nm$, while the torque of Gait 3 is $3.5Nm$.

velocity and step length increases as the hip torque grows, while the actuation has little influence on the efficiency.

B. Distribution of Different Gaits

Our experimental results indicated that ankle stiffness plays an important role in gait selection. Different ankle stiffness may result in different gaits with the same mechanical parameters. The manner of combination of the two ankle stiffness values K_a and K_b has a great influence on the walking gait. Fig. 6 shows the searched walking gaits for different ankle stiffness values. The results show that walking with both lower K_a and K_b converges to motion of Gait 1, while larger stiffness leads to Gait 2. The cyclic walking in Gait 3 is found when K_a is relatively small and K_b is large. There are also some transition regions in the K_a-K_b plane. The hybrid gaits in Fig. 6 refer to the following cases: (here we take "Gait 1 and Gait 2" for example): 1) Cyclic walking with Gait 1 and Gait 2 are both found at the same ankle stiffness. The initial conditions of the two gaits are different; 2) Gait 1 and Gait 2 alternatively appear in different steps of the walking.

C. Gait Transition

In this simulation, we evaluate the process of gait transition if the ankle stiffness is preset for a certain gait. During the simulation, the ankle stiffness $K_a = 40N/m$ and $K_b = 90N/m$, which indicates that the walker achieves stable walking in Gait 3. If we set the initial conditions of walking as Gait 2, after several steps, the walker will finally transit to Gait 3 where the walker can achieve most stable walking.

Fig. 7 shows the trajectory of the thigh during the transition process. If we set the ankle stiffness $K_a = 55N/m$ and $K_b = 100N/m$, according to the gait distribution result (see Fig. 6), the walker performs stable walking in not a single gait. Fig. 8 shows the results. One can find that the walking gait switches between Gait 2 and Gait 3. The walking transits between two limit cycles.

From the simulation results mentioned above, one can find that the ankle stiffness plays an important role in gait

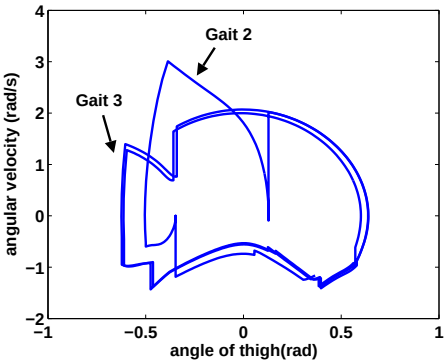

Fig. 7. Trajectory of the thigh during gait transition.

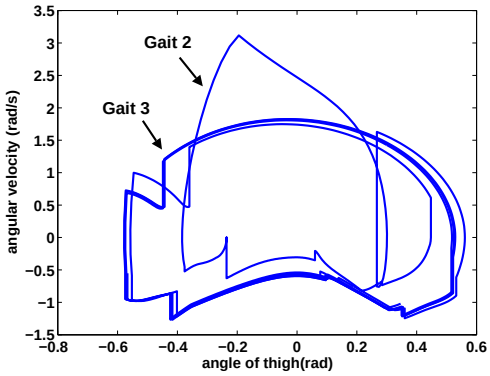

Fig. 8. Trajectory of the thigh during gait transition.

selection. The stiffness has great influence on the force states of the feet, which determine the constrain condition and phase switching of the model. Thus different ankle stiffness may result in different walking gaits. The gait distribution in the ankle stiffness plane (see Fig. 6) could be explained by the relation between the stiffness and the force states of the feet. Large K_b produces large ankle torque that pulls the heel of the trailing leg up before heel-strike of the leading leg, which leads to premature heel rise. Meanwhile, small K_a results in large average ankle torque in push-off phase. Thus the swing leg obtains large angular velocity to travel a long distance over one step. Consequently, the walker with large K_b and small K_a is easily to move to Gait 3. Smaller ankle stiffness results in small ankle joint torque. In this case, the trailing foot hardly loses contact with ground. Therefore, both small stiffness values are much possible to lead the walking to Gait 1. The ankle stiffness of Gait 2 is relatively larger. The result is that the trailing foot loses contact with ground before foot-strike of leading leg.

The study of the effects of ankle stiffness on motion characteristics also reveals the different roles that ankle stiffness plays in different gaits. In Gait 3 with large K_b and small K_a, ankle actuation provides large amount of energy to produce fast walking and long step length. Flexibility plays dominant effect in Gait 1. In Gait 2, ankle stiffness has a moderate value which obtains a balance of compliance and stiffness.

IV. Conclusion

In this paper, we have proposed a dynamic bipedal walking model with upper body, flat feet and compliant joints. The model realizes the three common walking gaits. Based on the proposed model, we investigated the effects of ankle stiffness on dynamic walking. The simulation results indicate that ankle stiffness has great influence on gait selection.

References

[1] D. Schmitt, Insights into the evolution of human bipedalism from experimental studies of humans and other primates, *Journal of Experimental Biology*, vol. 206, pp.1437-48, 2003.

[2] J. R. Skoyles, Human balance, the evolution of bipedalism and dysequilibrium syndrome, *Medical Hypotheses*, vol. 66, pp. 1060-1068, 2006.

[3] T. McGeer, Passive dynamic walking, *International Journal of Robotics Research*, vol. 9, pp. 68-82, 1990.

[4] M. Garcia, A. Chatterjee, A. Ruina, M. Coleman, The simplest walking model: stability, complexity, and scaling, *ASME Journal Biomechanical Engineering*, vol. 120, pp. 281-288, 1998.

[5] A. D. Kuo, Energetics of actively powered locomotion using the simplest walking model, *ASME Journal Biomechanical Engineering*, vol. 124, pp. 113-120, 2002.

[6] A. Ruina, J. E. A. Bertram, M. Srinivasan, A collisional model of the energetic cost of support work qualitatively explains leg sequencing in walking and galloping, pseudo-elastic leg behavior in running and the walk-to-run transition, *Journal of Theoretical Biology*, vol. 237, no. 2, pp. 170-192, 2005.

[7] M. Kwan, M. Hubbard, Optimal foot shape for a passive dynamic biped, *Journal of Theoretical Biology*, vol. 248, pp. 331-339, 2007.

[8] S. Mochon, T. A. McMahon, Ballistic walking, *J. Biomech.* **13**(1), 49-57 (1980).

[9] D. G. E. Hoboelen, M. Wisse, Ankle actuation for limit cycle walkers, *International Journal of Robotics Research*, vol. 27, no. 6, pp. 709-735, 2008.

[10] Q. Wang, Y. Huang, L. Wang, Passive dynamic walking with flat feet and ankle compliance, *Robotica*, vol. 28, pp. 413-425, 2010.

[11] Q. Wang, Y. Huang, J. Zhu, L. Wang, D. Lv, Effects of foot shape on energetic efficiency and dynamic stability of passive dynamic biped with upper body, *International Journal of Humanoid Robottics*, vol. 7, no. 2, pp. 295-313, 2010.

[12] M. Wisse, A. L. Schwab, F. C. T. Van der Helm, Passive dynamic walking model with upper body, *Robotica*, vol. 22, pp. 681-688, 2004.

[13] C. Frigo, P. Crenna, L. M. Jensen, Moment-angle relationship at lower limb joints during human walking at different velocities, *Journal of Electromyography and Kinesiology*, vol. 6, no. 3, pp. 177-190, 1996.

[14] T. Sinkjaer, E. Toft, S. Andreassen, B. C. Hornemann, Muscle stiffness in human ankle dorsiflexors: intrinsic and reflex components, *Journal of Neurophysiology*, vol. 60, no. 3, pp. 1110-1120, 1988.

[15] I. W. Hunter, R. E. Kearney, Dynamics of human ankle stiffness: variation with mean ankle torque, *Journal of Biomechanics*, vol. 15, no. 10, pp. 747-752, 1982.